A Hybrid Level-Set LES / CAA Method for Thermoacoustic Analyses

Konrad Pausch[1], Sohel Herff[1], Wolfgang Schröder[1,2]

[1] *Institute of Aerodynamics, RWTH Aachen University, 52062 Aachen, Germany, Mail: k.pausch@aia.rwth-aachen.de*

[2] *JARA High-Performance Computing, Forschungszentrum Jülich, 52425 Jülich*

Abstract

To develop modeling strategies that help to avoid combustion instabilities in future combustor systems, a deeper understanding of the mechanisms that generate combustion noise is needed. Due to the disparity of the involved scales a hybrid approach is used for the investigation. In the first step the flow field is computed using large-eddy simulation (LES) that applies a combined G-equation progress variable approach by Moureau et al. [20] to model chemical reactions. In the second step the acoustic perturbation equations (APE) by Ewert and Schröder [4] are solved to determine the acoustic field based on the sources and the mean flow computed from the LES data. The method is used to investigate an experimental burner configuration by Nawroth et al. [21]. The numerical and experimental acoustics are in good agreement.

Introduction

Since jet noise and fan noise are reduced through recent technological progress [3], combustion noise becomes an increasingly important contributor to the overall sound emission of jet aero engines. Furthermore, a deeper understanding of combustion noise source mechanisms is required for the development of highly efficient low-emission gas turbines, since the lean-premixed regime is prone to thermoacoustic instabilities. Such instabilities are characterized by the amplified interaction between acoustic pressure and the flame's unsteady heat release and can ultimately lead to the structural failure of the burner assembly. [17].

Two distinct mechanisms define the generation of combustion noise [3]: Direct combustion noise generated in the combustion chamber and indirect combustion noise generated due to the acceleration of entropy inhomogeneities, i.e., hot spots convected through a nozzle or a turbine stage [31, 18, 1]. The spectral shape of direct combustion noise from open flames has been studied experimentally [16, 25] with respect to fuel, flow parameters, and the burner geometry, numerically [28], and empirically [32]. Still, the mechanisms of the sound generation remain unknown and further detailed studies on the acoustic source terms are necessary. In classical theory, the sound generation is often associated with the flame's unsteady rate of heat release acting as a distribution of monopole sound sources [34, 12], but there is no general justification that this is the dominant sound source independent from the gas mixture, flow conditions, or burner geometry.

Nawroth et al. [21] have designed a generic experimental setup to fundamentally investigate the generation of combustion noise of lean-premixed turbulent flames in an unconfined environment. This setup is studied numerically with a hybrid LES/CAA approach by solving the acoustic perturbation equations (APE) [4], which have been extended [2, 15] for the analysis of combustion noise based on LES data. Based on an experimental validation of the numerically predicted acoustics, the numerical data will be used to analyze the acoustic source mechanisms and their near-field radiation in detail.

Numerical method

The hybrid concept defines the numerical analysis. In the first step, the compressible Navier-Stokes equations for a three-dimensional unsteady reacting flow are solved by means of large-eddy simulation coupled with a combined G-equation progress variable approach by Moureau et al. [20] to model the combustion process. The G-equation approach is used to describe the motion of the inner-layer temperature contour of the flame, where the contour represents the zero-level set, i.e., the $G = G_0 = 0$ contour, of a three-dimensional function $G(x; y; z; t)$. This function is defined to be the signed-distance function of the inner-layer temperature contour. The evolution of this zero level-set contour is defined by the G-equation [23, 26]

$$\frac{\partial \check{G}}{\partial t} + \left(\tilde{\boldsymbol{v}} + \frac{\rho_{\infty,u}}{\bar{\rho}} \hat{\check{s}}_{t,u} \check{\boldsymbol{n}} \right) \cdot \nabla \check{G} = 0, \tag{1}$$

$$\check{\boldsymbol{n}} = -\frac{1}{|\nabla \check{G}|} \left(\partial \check{G}/\partial x,\ \partial \check{G}/\partial y,\ \partial \check{G}/\partial z \right)^T, \tag{2}$$

where the symbol $\check{\cdot}$ indicates a variable defined at the filtered flame front location $\hat{\check{\boldsymbol{x}}}_f$ such that $\check{G}(x,t) = G_0$. The symbol $\hat{\cdot}$ represents variables which are filtered by the surface integral over the resolved flame front, whereas $\tilde{\cdot}$ represents Favre filtered and $\bar{\cdot}$ spatially filtered variables. The quantity $\tilde{\boldsymbol{v}}$ is the Favre filtered flow velocity, $\rho_{\infty,u}$ the freestream density in the unburnt gas, $\bar{\rho}$ is the spatially filtered density, and $\check{\boldsymbol{n}}$ the normal vector at $\hat{\check{\boldsymbol{x}}}_f$ pointing towards the unburnt gas mixture. In the present study, the flame speed is modeled by [23, 26]

$$\hat{\check{s}}_{t,u} = \hat{\check{s}}_{L,0} \left[1 - l_c \check{\kappa} \right] + s_T, \tag{3}$$

where $\hat{\check{s}}_{L,0}$ is the laminar flame speed and l_c is the Markstein length which allows the flame speed to vary with the flame front curvature $\check{\kappa} = \nabla \cdot \check{\boldsymbol{n}}$ [19, 24]. The second term on the right-hand side of Eq. (3) is a modeling term and arises when flame thickening is considered in LES computations [23]. This formulation is valid in the corrugated as well as the thin reaction zone regime as demonstrated in [23]. For more details with respect to the combustion

solver and the used LES model, the reader is referred to [26, 28, 23, 9]. This combustion model has been shown to satisfactorily capture the dynamics of the flame surface for several canonical problems, e.g., flame-vortex interaction [20, 9], Darrieus-Landau instability [27], mean heat release rate distribution, and mean turbulent mass consumption speed [26].

An unstructured Cartesian grid flow solver based on a strictly conservative finite-volume methodology [7, 8, 9] is used for the numerical solution. The convective terms are discretized by a second-order accurate modified low-dissipation AUSM scheme and the viscous terms are approximated by second-order accurate central differences. Time-integration is done by a third-order total-variation diminishing (TVD) Runge-Kutta scheme [26]. A conservative cut-cell technique captures arbitrary embedded boundaries [30, 29].

In the second step, the acoustic field is computed using the acoustic perturbation equations by Ewert and Schröder [4]. The left-hand side corresponds to the filtered linearized Euler equations extended for a non-uniform mean flow field describing acoustic wave propagation into the far field. The right-hand side consists of the source terms resulting from the linearization of the governing equations of viscous flow and determines the acoustic emission. In the APE-4 formulation the perturbation density is eliminated by combining the energy and the continuity equation.

$$\frac{\partial p^a}{\partial t} + \overline{c^2}\boldsymbol{\nabla}\cdot\left(\overline{\rho}\boldsymbol{v}^a + \overline{\boldsymbol{v}}\frac{p^a}{\overline{c^2}}\right) = \overline{c^2}q_c + q_e - \underbrace{\overline{c^2}\boldsymbol{\nabla}\cdot(\overline{\boldsymbol{v}}\rho_e)}_{q_{c\&e}} \quad (4)$$

$$\frac{\partial \boldsymbol{v}^a}{\partial t} + \boldsymbol{\nabla}\left(\overline{\boldsymbol{v}}\cdot\boldsymbol{v}^a\right) + \boldsymbol{\nabla}\left(\frac{p^a}{\overline{\rho}}\right) = \boldsymbol{q_m}. \quad (5)$$

resulting in an additional source term $q_{c\&e}$ besides the continuity source term q_c, the momentum source term q_m, and the energy source term q_e. Due to the extension to a non-uniform mean flow field convection and refraction effects are taken into account by the left-hand side operator. The results from the large-eddy simulation determine the mean flow quantities and the sources

$$q_c = -\boldsymbol{\nabla}\cdot(\rho'\boldsymbol{v}')' \quad (6)$$

$$\boldsymbol{q_m} = (\boldsymbol{\omega}\times\boldsymbol{v})' - \boldsymbol{\nabla}k' + \boldsymbol{\nabla}\left(\frac{p'}{\overline{\rho}}\right) - \left(\frac{\boldsymbol{\nabla}p}{\rho}\right)' + \underbrace{\left(\frac{\boldsymbol{\nabla}\cdot\underline{\boldsymbol{\tau}}}{\rho}\right)'}_{neglected} \quad (7)$$

$$q_e = -\overline{c^2}\frac{\partial {\rho_e}'}{\partial t} = \frac{\partial p'}{\partial t} - \overline{c^2}\frac{\partial \rho'}{\partial t}, \quad (8)$$

which further include the vorticity ω, the turbulent kinetic energy k, and the stress tensor $\underline{\boldsymbol{\tau}}$. In the case of combustion noise, the energy source term q_e usually dominates the acoustic field [6, 5, 22]. For further analysis, it is rewritten using substantial derivatives

$$q_e = \underbrace{\left(\frac{\mathrm{D}p}{\mathrm{D}t} - c^2\frac{\mathrm{D}\rho}{\mathrm{D}t}\right)'}_{q_{e,1}} + \underbrace{\left(\left(c^2\right)'\frac{\partial\rho}{\partial t}\right)'}_{q_{e,2}} + \underbrace{\left(\boldsymbol{v}\cdot\left(c^2\boldsymbol{\nabla}\rho - \boldsymbol{\nabla}p\right)\right)'}_{q_{e,3}}. \quad (9)$$

to identify $q_{e,3}$ as indirect combustion noise due to acceleration of entropy inhomogeneities, $q_{e,2}$ as noise source due to intermittency effects caused by sudden changes in the speed of sound, and the substantial pressure-density relation $q_{e,1}$, which includes the effect of fluctuating heat release [5]. The APE-1 system contains a source filtered right-hand side, i.e., the source terms of the APE-1 system excite acoustic modes only [4]. Since the APE-4 system is derived by rewriting the governing equations such that the left-hand side corresponds to the APE-1 operator, the source terms appearing on the right-hand side are not filtered and also support vorticity modes. However, unlike the linearized Euler equations the APE system is still stable [4]. Outside the source region, the right-hand side vanishes and the fluctuations in pressure and velocity computed by the APE operator contain only the acoustic mode.

The acoustic perturbation equations are discretized in space using a 9-point 6th-order dispersion-relation preserving summation by parts scheme (SBP-DRP) [13]. The temporal integration is done by an alternating 5-6 stage low-dispersion low-dissipation Runge-Kutta scheme (LDDRK) [11]. A radiation boundary condition is used on the domain boundaries to avoid reflections. [33]

Application to an experimental burner configuration

The hybrid approach is used to study an experimental burner configuration from TU Berlin [21] that is designed for the fundamental investigation of combustion noise of lean-premixed flames in an anechoic environment. The setup is depicted in figure 1. Note that the premixed methane-air mixture is injected through six annular drillings located at the bottom of the burner plenum. Therefore, to accurately reproduce the experimental turbulent flow field in the numerical simulation, the full burner plenum with the radial injection is included in the LES domain leading to $87\cdot10^6$ grid points. The investigated setup has a Reynolds number of $Re = 10,000$ and a Mach number of $M = 0.013$ based on the diameter d and the mean flow conditions at the burner exit. The equivalence ratio is $\phi = 0.7$. The source terms on the right-hand side of the APE-4 system given by equations 4 and 5 are computed in the source region that is defined by a cylindrical domain ranging from 0 to $5d$ downstream of the burner exit plane with a diameter of $2d$.

In a previous study [10], the flow statistics of the cold jet was shown to be in good agreement with the experimental data and the full plenum computation of the cold jet revealed the existence of acoustic modes within the

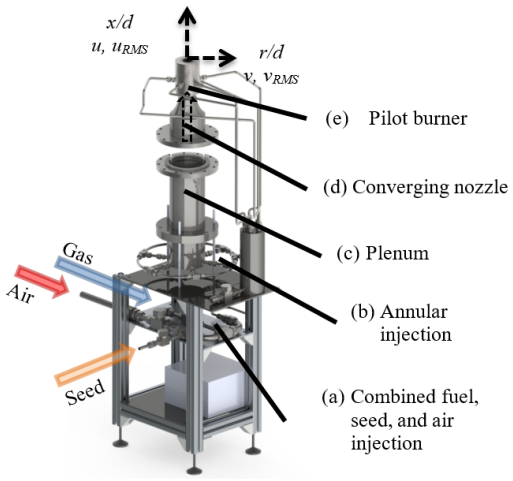

Figure 1: Schematic of the experimental setup by Nawroth et al. [21].

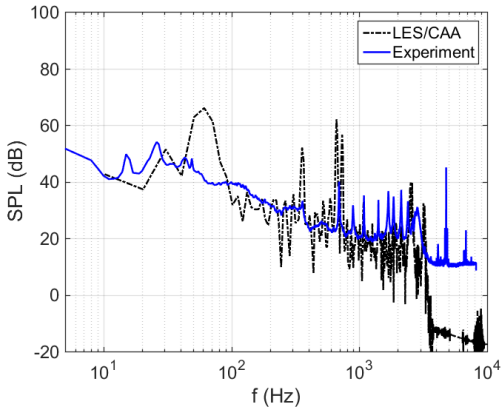

Figure 2: Acoustic spectra at far-field microphone position $x = 0D, r = 30D$.

burner plenum. The current study extends the analysis from acoustics of the cold flow to the acoustics of the reacting flow. In figure 2 the acoustic spectrum obtained by the CAA simulation at the far-field microphone position $x = 0D, r = 30D$ shows several peaks at the frequencies $f = 60Hz$, $f = 360Hz$, and $f = 720Hz$. Similar peaks are also observed in the Fourier transformed LES pressure inside the plenum given in figure 3. It is concluded that acoustic modes within the burner plenum excite the flame leading to the peaks observed in the far-field spectrum. The experimental results also show peaks at $f = 360Hz$ and $f = 720Hz$, however, there is no distinct mode found at $f = 60Hz$. The overall broadband acoustic spectra of the experiment and CAA simulation are quantitatively in good agreement.
The numerical data will be used for a detailed analysis of the acoustic source mechanisms and radiation characteristics.

Conclusion

A hybrid method for the analysis of combustion noise has been presented. The reacting flow is computed by means of an LES that applies a combined G-equation

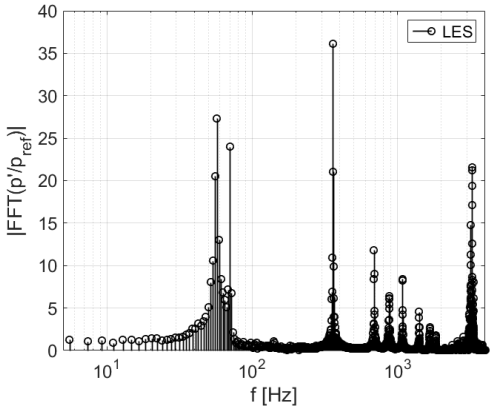

Figure 3: Fourier transformed LES pressure signal in burner plenum

progress variable approach by Moureau et al. [20]. The acoustic field is determined by solving the acoustic perturbation equations in the APE-4 formulation based on the sources and the mean flow field computed from the LES solution. An application of this method to an experimentally investigated burner configuration shows a convincing agreement between the far-field acoustic pressure obtained by the CAA simulation and by the experiment. The hybrid concept allows to investigate the single thermoacoustic and flow noise source mechanisms by evaluating the contributions of the various APE-4 source terms to the acoustic pressure signal and their radiation characteristics.

Acknowledgments

This study was supported by the DFG Combustion Noise grant SCHR 309/43. We acknowledge PRACE for awarding us access to resource JUQUEEN [14] based in Germany at Jülich Supercomputing Centre.

References

[1] F. Bake, C. Richter, B. Mühlbauer, N. Kings, I. Röhle, F. Thiele, and B. Noll. The entropy wave generator (EWG): a reference case on entropy noise. *J. Sound Vib.*, 326(3):574–598, 2009.

[2] P. T. Bui, M. Meinke, W. Schröder, F. Flemming, A. Sadiki, and J. Janicka. A hybrid method for combustion noise based on LES and APE. *AIAA Paper*. 2005-3014, 2005.

[3] A. P. Dowling and Y. Mahmoudi. Combustion noise. *P. Combust. Inst.*, 35:65–100, 2015.

[4] R. Ewert and W. Schröder. Acoustic perturbation equations based on flow decomposition via source filtering. *J. Comput. Phys.*, 188:365–398, 2003.

[5] G. Geiser, A. Hosseinzadeh, H. Nawroth, F. Zhang, H. Bockhorn, P. Habisreuther, J. Janicka, C. O. Paschereit, and W. Schröder. Thermoacoustics of a turbulent premixed flame. *AIAA Paper*. 2014-2476, 2014.

[6] G. Geiser, S. Schlimpert, and W. Schröder. Thermoacoustical noise induced by laminar flame annihilation at varying flame thicknesses. *AIAA Paper*. 2012-2093, 2012.

[7] D. Hartmann, M. Meinke, and W. Schröder. An adaptive multilevel multigrid formulation for cartesian hierarchical grid methods. *Comp. Fluids*, 37:1103–1125. 2008.

[8] D. Hartmann, M. Meinke, and W. Schröder. The constrained reinitialization equation for level set methods. *J. Comput. Phys.*, 229:1514–1535. 2010.

[9] D. Hartmann, M. Meinke, and W. Schröder. A level-set based adaptive-grid method for premixed combustion. *Combust. Flame*, 158(7):1318–1339. 2011.

[10] S. Herff, K. Pausch, H. Nawroth, S. Schlimpert, C. Paschereit, and W. Schröder. Impact of turbulent inflow distributions on combustion noise of lean-premixed flames. *AIAA Paper*.

[11] F. Hu, M. Hussaini, and J. Manthey. Low-dissipation and low-dispersion Runge-Kutta schemes for computational acoustics. *J. Comput. Phys.*, 124:177–197, 1996.

[12] I. R. Hurle, R. B. Price, T. M. Sugden, and A. Thomas. Sound emission from open turbulent premixed flames. *P. R. Soc. London*, 303:409–427, 1968.

[13] S. Johansson. High order finite difference operators with the summation by parts property based on DRP schemes, 2004.

[14] Jülich Supercomputing Centre. JUQUEEN: IBM Blue Gene/Q Supercomputer System at the Jülich Supercomputing Centre. *Journal of large-scale research facilities*, 1(A1), 2015.

[15] S. Koh, G. Geiser, and W. Schröder. Reformulation of acoustic entropy source terms. *AIAA Paper*. 2011-2927, 2011.

[16] S. Kotake and K. Takamoto. Combustion noise: effects of the shape and size of burner nozzle. *J. Sound Vib.*, 112(2):345–354, 1987.

[17] T. Lieuwen and V. Yang. *Combustion Instabilities in Gas Turbine Engines: Operational Experience, Fundamental Mechanisms, and Modeling*, volume 210. AIAA, Reston, VA, 2005.

[18] F. Marble and S. Candel. Acoustic disturbance from gas non-uniformities convected through a nozzle. *J. Sound Vib.*, 55:225–243, 1977.

[19] G. Markstein. *Nonsteady flame propagation*, volume 75. Pergamon Press, New York, 1964.

[20] V. Moureau, B. Fiorina, and H. Pitsch. A level set formulation for premixed combustion LES considering the turbulent flame structure. *Combust. Flame*, 156(4):801–812. 2009.

[21] H. Nawroth and C. O. Paschereit. High-speed flow field measurements of turbulent jet flames undergoing shear layer manipulation. *AIAA Paper*. 2016-1841, 2016.

[22] K. Pausch, S. Schlimpert, S. R. Koh, J. Grimmen, and W. Schröder. The effect of flame thickening on the acoustic emission in turbulent combustion. *AIAA Paper*.

[23] H. Pitsch. A consistent level set formulation for large-eddy simulation of premixed turbulent combustion. *Combust. Flame*, 143(4):587–598. 2005.

[24] T. Poinsot, T. Echekki, and M. G. Mungal. A study of the laminar flame tip and implications for premixed turbulent combustion. *Combust. Sci. Technol.*, 81(1-3):45–73, 1992.

[25] R. Rajaram and T. Lieuwen. Acoustic radiation from turbulent premixed flames. *J. Fluid Mech.*, 637:357–385, 2009.

[26] S. Schlimpert, A. Feldhusen, J. H. Grimmen, B. Roidl, M. Meinke, and W. Schröder. Hydrodynamic instability and shear layer effects in turbulent premixed combustion. *Phys. Fluids*, 28(1), 2016.

[27] S. Schlimpert, S. Hemchandra, M. Meinke, and W. Schröder. Hydrodynamic instability and shear layer effect on the response of an acoustically excited laminar premixed flame. *Combust. Flame*, 162(2):345–367, 2015.

[28] S. Schlimpert, S. R. Koh, K. Pausch, M. Meinke, and W. Schröder. Analysis of combustion noise of a turbulent premixed slot jet flame. *Combust. Flame*, 175(1):292–306, 2017.

[29] L. Schneiders, C. Günther, M. Meinke, and W. Schröder. An efficient conservative cut-cell method for rigid bodies interacting with viscous compressible flows. *J. Comput. Phys.*, 311:62–68, 2016.

[30] L. Schneiders, D. Hartmann, M. Meinke, and W. Schröder. An accurate moving boundary formulation in cut-cell methods. *J. Comput. Phys.*, 235:786–809, 2013.

[31] W. Strahle. Combustion noise. *Prog. Energy Combust. Sci.*, 4:157–176, 1978.

[32] C. K. W. Tam. The spectral shape of combustion noise. *International Journal of Aeroacoustics*, 14:431–456, 2015.

[33] C. K. W. Tam and J. C. Webb. Dispersion-relation-preserving finite difference schemes for computational acoustics. *J. Comput. Phys.*, 107:262–281, 1993.

[34] A. Thomas and G. T. Williams. Flame noise: sound emission from spark-ignited bubbles of combustible gas. *Proceedings of the Royal Society of London. Series A. Mathematical and Physical Sciences*, 294(1439):449–466, 1966.